Supplementary table 1: Antibodies use the study for flow cytometry

Company	Antibody	Target species	Clone	Fluorochrome
BioLegend	hCD45	human	HI30	APC-Cy7
BioLegend	CD19	human	HIB19	PB
BioLegend	CD20	human	2H7	PB
BD	mCD45	mouse	30-F11	V500
BioLegend	CD3	human	OKT3	BV711
BioLegend	CD14	human	HCD14	APC
BioLegend	HLA-DR	human	L243	PerCP-Cy5.5
BD	CD11c	human	B-LY6	PE-CF594
BD	CD123	human	7G3	BUV395
BioLegend	CD1c	human	L161	AF700
BioLegend	CD141	human	M80	PE-Cy7
BD	CD11b	human	ICRF44	BV650

Supplementary table 2: Oligonucleotides used in this study

Name	**Sequence**	**Description**
DROSHA-f	TTGGAACGAGTAGGCTTCGT	Human *DROSHA* qPCR forward primer
DROSHA-r	CAGGTGCTGTCCTCATCAGA	Human *DROSHA* qPCR reverse primer
DICER-f	GCTGTGTACGATTGGCTGAA	Human *DICER* qPCR forward primer
DICER-r	GGTAGCACTGCCTTCGTTTC	Human *DICER* qPCR reverse primer
MYL9-f	CTTCACCATGTTCCTCACCA	Human *MYL9* qPCR forward primer
MYL9-r	CCGGTACATCTCGTCCACTT	Human *MYL9* qPCR reverse primer at position 481
l2_00017631-f	CCAGACCCCTCCACTGTAAA	Human *TCONS_l2_00017631* qPCR forward primer
l2_00017631-r	AAACTGGAATGGCCTGTCAC	Human *TCONS_l2_00017631* qPCR reverse primer
GAPDH-f	GTGGACCTGACCTGCCGTCT	Human *GAPDH* qPCR forward primer
GADPH-r	GGAGGAGTGGGTGTCGCTGT	Human *GAPDH* qPCR reverse primer
5’ adaptor	ACTCTTTCCCTACACGACGC	Forward primer against RNA oligo adaptor
MYL9-213	TGCAGGTCCTCCTTGTCAAT	*MYL9* reverse primer at position 213
MYL9-257	GGTATTCGTCTGTGGGGTTC	*MYL9* reverse primer at position 257
MYL9-372	GCAAAGGCGTTGCGAATCAC	*MYL9* reverse primer at position 372

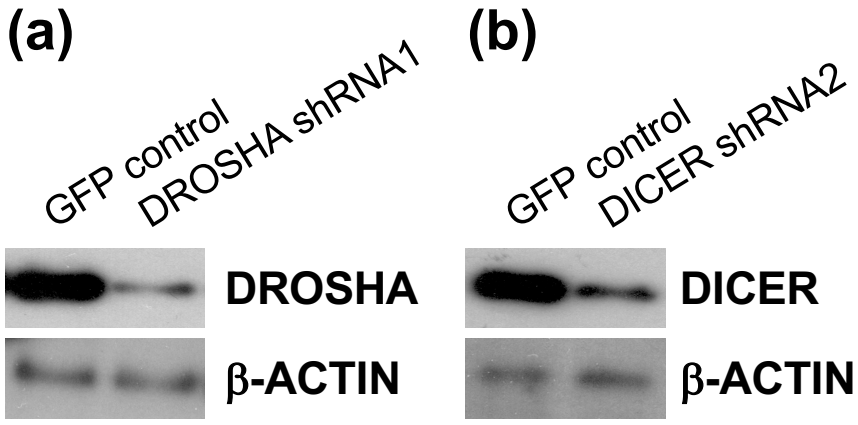

Supplementary Figure 1: Detection of DROSHA and DICER protein levels following shRNA-mediated knockdown. Jurkat cells were transduced with lentiviral shRNAs against DROSHA, DICER or an empty vector. The transduced cells (GFP+) were sorted and analysed for **(a)** DROSHA or **(b)** DICER protein by Western blotting. Separate gels were run for the β-ACTIN loading controls due to differences in detection sensitivities. Lysates from 5×10^6 cells were loaded for the DROSHA and DICER blots, while lysates from 2×10^5 cells were loaded for the β-ACTIN blots. A representative of two experiments is shown.

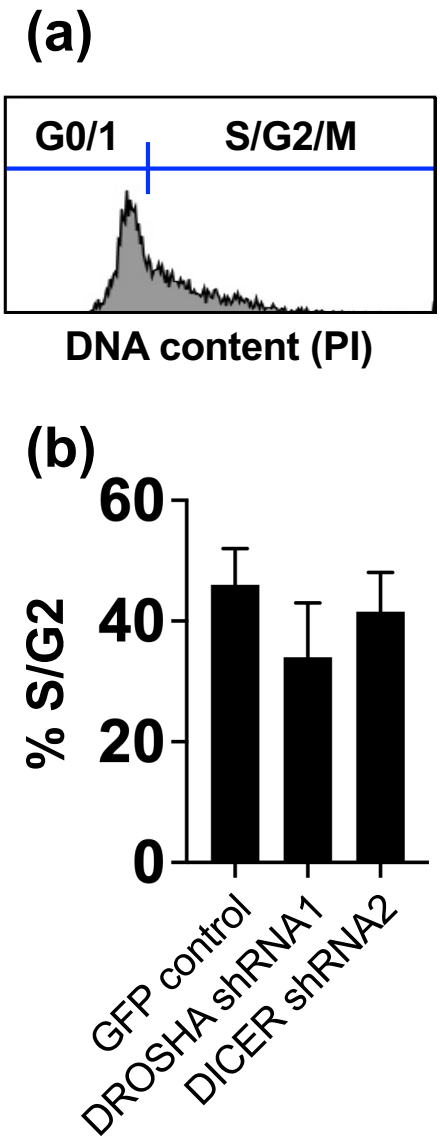

Supplementary Figure 2: Cell cycle analysis of CD34$^+$ HSCs following DROSHA and DICER knockdown. (a) Cord blood CD34$^+$ cells were transduced with lentiviral shRNAs against DROSHA or DICER, or an empty viral (GFP only) control. After 3 days, the GFP$^+$ transduced cells were sorted to purity and expanded for a further 5 days, in culture. The cells were then analysed for cell cycle status by measuring DNA content (propidium iodide staining). **(b)** Shown is the mean ± S.EM of two experiments measuring the percentage of cells in S/G2/M as an indicator of proliferation.

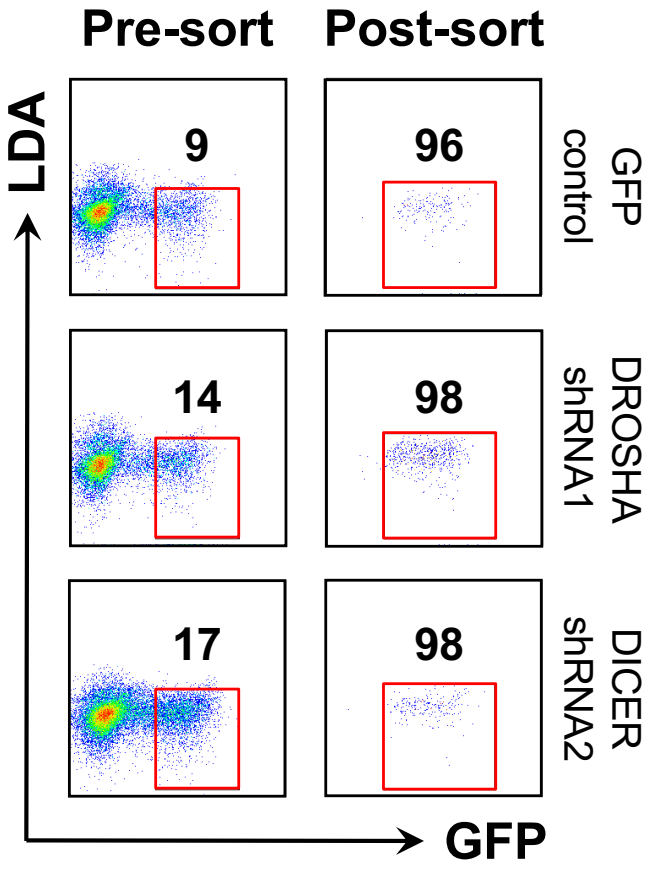

Supplementary Figure 3: Sorting of transduced CD34⁺ HSCs for engraftment into NSG-SGM3 mice. Cord blood CD34⁺ cells were transduced with lentiviral shRNAs against DROSHA or DICER, or an empty viral (GFP only) control. After 3 days, the GFP⁺ transduced cells were sorted to purity for engraftment into NSG-SGM3 mice. Typical percentages of GFP⁺ cells pre- and post-sort are indicated.

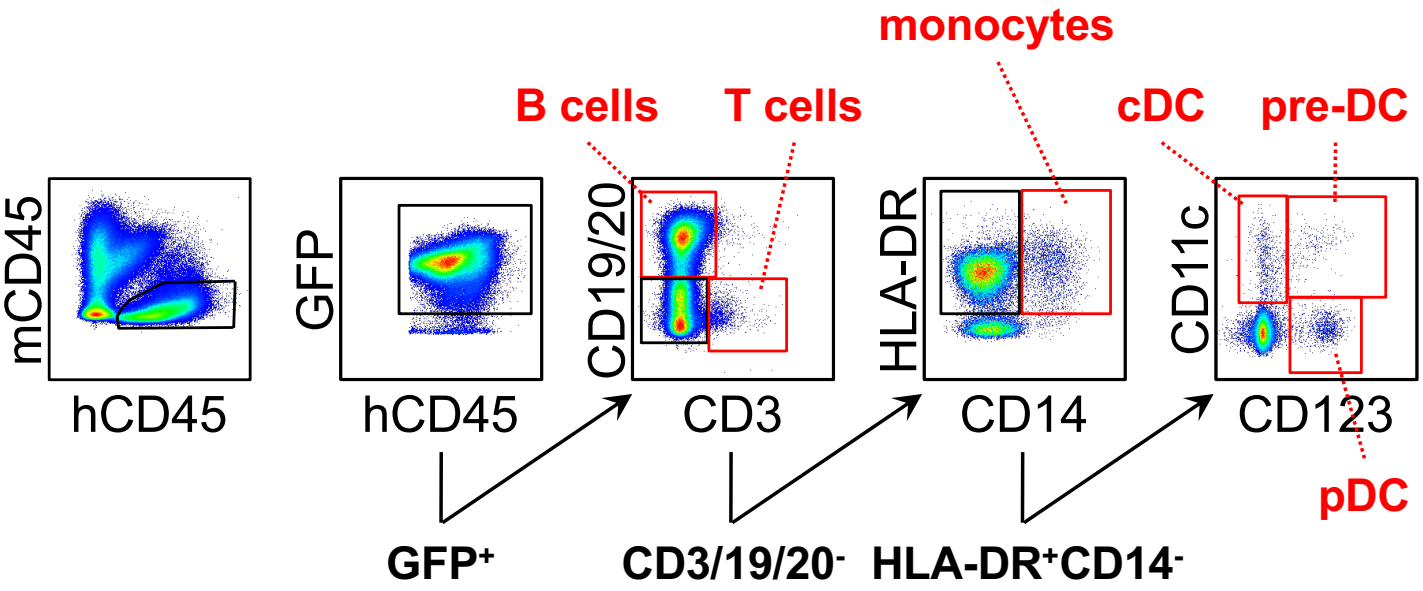

Supplementary Figure 4: Gating strategy for analysing humanized mice Shown is a representative flow cytometric analysis of the spleen for cells derived from the transduced cord blood $CD34^+$ cells. Expression of hCD45 and GFP identifies cells derived from the engrafted transduced human $CD34^+$ cells. These are then subdivided into $CD19^+CD20^+$ B cells, $CD3^+$ T cells, HLA-DR^+CD14^+ monocytes, HLA-$DR^+CD11c^+CD123^-$ conventional dendritic cells (cDC), HLA-$DR^+CD11c^-CD123^+$ plasmacytoid dendritic cells (pDC) and HLA-$DR^+CD11c^+CD123^+$ pre-DC.